Research Journal of Applied Sciences, Engineering and Technology 7(19): 4088-4094, 2014
DOI:10.19026/rjaset.7.771
ISSN: 2040-7459; e-ISSN: 2040-7467

Submitted: December 04, 2013 Accepted: January 01, 2014 Published: May 15, 2014

Research Article

A Statistical Approach of Texton Based Texture Classification Using LPboosting Classifier

[1]C. Vivek and [2]S. Audithan
[1]PRIST University, Tanjore, Tamilnadu, India
[2]Department of Computer Science and Engineering, PRIST University, Tamilnadu, India

Abstract: The aim of the study in this research deals with the accurate texture classification and the image texture analysis has a voluminous errand prospective in real world applications. In this study, the texton co-occurrence matrix applied to the Broadatz database images that derive the template texton grid images and it undergoes to the discrete shearlet transform to decompose the image. The entropy lineage parameters of redundant and interpolate at a certain point which congregating adjacent regions based on geometric properties then the classification is apprehended by comparing the similarity between the estimated distributions of all detail sub bands through the strong LP boosting classification with various weak classifier configurations. We show that the resulted texture features while incurring the maximum of the discriminative information. Our hybrid classification method significantly outperforms the existing texture descriptors and stipulates classification accuracy in the state-of-the-art real world imaging applications.

Keywords: LPboost classifier, shearlet transform, texton co-occurrence matrix, texture image classification, weak classification

INTRODUCTION

The textures in the image or texels are the repetitive patterns or spatial sequence to analyze all real environment objects as images by Randen and Husoy (1999). The spatial analysis in the small Texel region or micro-textures is complicated with the existing statistical approaches such as Gauss-Markov random fields, second-order statistics or local linear descriptor transform based on Smith and Chang (1994). It discards the templates of internal frequency varying regions. The spatial filter banks such as Gabor, S-filter and Gaussian fails to correlate the texture features for evaluating the features by Unser (1995). The statistical textural features in estimating the spatial relationship of various types of data sets of aerial and satellite image analyzed by Haralick *et al*. (1973). The calculation of spectral features of texture image of terrain based on power spectrum to estimate the roughness in the ring and wedge based region yields inaccurate towards different type of data determined by Chen and Young (1982). Later, the discrete Broadatz textures are characterized to yield optimal transform from the set of histogram obtained through the neighbourhood pixel or co-occurrence based classification that results in overlapping applied by Unser (1986). By using wavelet transform to extract the multi-component texture method improves orthogonality but highly time consuming for due to multi-scale strategy. The images with different features are marked as indices based on relative similarity based on the research by Monay and Gatica-Perez (2007). The Content Based Image Retrieval (CBIR) for object or feature analysis exploit much research developments with application. Among them, the multi-texton histogram integrates with the co-occurrence matrix based on Julesz's textons theory to describe image features by Liu *et al*. (2011). Feature extraction method consists of gray level co-occurrence matrix and GMRF features. The classification is done by using Support Vector Machine (SVM). A detailed literature review is presented by Tou *et al*. (2009) for the classification of texture images based on various feature extraction techniques. In our previous work (Vivek and Audithan, 2014) that we integrated the characterization of textures based on Discrete Shearlet Transform (DST) by extracting entropy measure and to classify the given Brodatz database texture image using K-Nearest Neighbor (KNN) classifier by Fang *et al*. (2010). Although such adaptation improves the classification accuracy, it also severely increases the feature space complexity. Similarly, the an exclusive machine learning algorithm with strong supervised LP Boost classifier to train the ADNI database of MR images in a hyper-plane shows improved in classification compared with other methods that developed by Fang *et al*. (2011). Similarly, the LP Boost algorithm optimized for weak classifier while ignoring strong classifier through mini-max theory that revokes on the edge constraint shows higher convergence rate and accuracy for real world

Corresponding Author: C. Vivek, PRIST University, Tanjore, Tamilnadu, India

applications. Later, the same algorithm updated with strong classifier with the limited range that the training set of 5-fold-cross validation shows higher accuracy in the research by Easley *et al*. (2008) and Liu *et al*. (2010). Thus, we propose the combination of multi-texton histogram with the Discrete Shearlet Transform (DST) to discriminate the Brodatz album based on feature extraction and then it undergoes classification with the mini-max theory based LPboost classifier the accuracy of this system very well compared to other state of art techniques.

TEXTON CO-OCCURRENCE MATRIX

The overall combination of the proposed system diagram is given in Fig. 1. In a gray level image, the Texton Co-occurrence Matrix (TCM) differentiates the features of pixel based on the interrelation to the textons. Let g be the unit vector corresponding to the G of the gray level in the image, then the following vectors co-ordinate with the function f (x, y) that developed by Julesz (1981):

$$u = \frac{\partial G}{\partial x} g \tag{1}$$

$$v = \frac{\partial G}{\partial y} g \tag{2}$$

The dot products to the above vectors are given below:

$$g_{xx} = u^{\mathrm{T}} u = \left| \frac{\partial G}{\partial x} \right|^2 \tag{3}$$

$$g_{yy} = v^{\mathrm{T}} v = \left| \frac{\partial G}{\partial y} \right|^2 \tag{4}$$

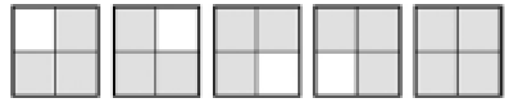

Fig. 1: Texton templates with five unique types

$$g_{xy} = u^{\mathrm{T}} v = \frac{\partial G}{\partial x} \bullet \frac{\partial G}{\partial y} \tag{5}$$

The θ (x, y) is the direction that changes with the vectors:

$$\theta(x, y) = \frac{1}{2} \tan^{-1} [\frac{2 g_{xy}}{(g_{xx} - g_{yy})}] \tag{6}$$

To identify the value ranges C (x, y) from lower value to higher value of 0 to 255, the G (x, y) is given below:

$$\mathrm{G}(x, y) = \{\frac{1}{2}[(g_{xx} + g_{yy}) + (g_{xx} - g_{yy}) \cos 2\theta + 2 g_{xy} \sin 2\theta]\}^{\frac{1}{2}} \tag{7}$$

The texton templates consist of five types of unique frames to identify the textons that illustrated in Fig. 2.

To identify the texton in the original image, the texton templates are morphed the input image on various texton locations that generate the five unique combinations of texton component images. Finally, the component images are combined together into texton identified image by enumerating the boundary for all morphed regions that shown in Fig. 3.

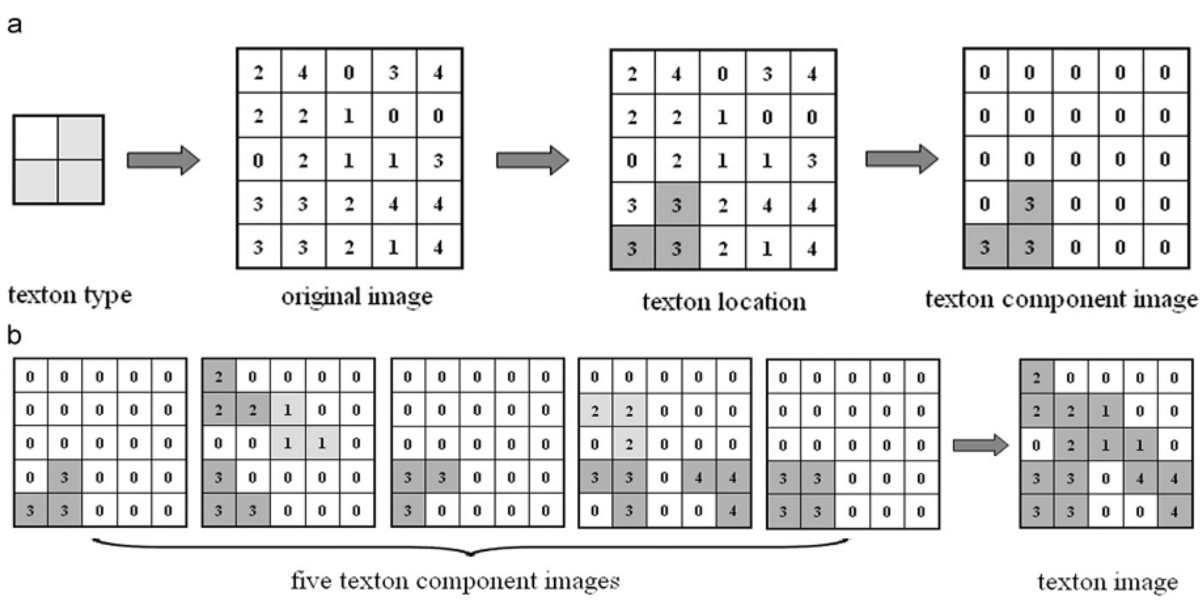

Fig. 2: The process of texton identification in TCM, (a) texton component identification, (b) generated texton image

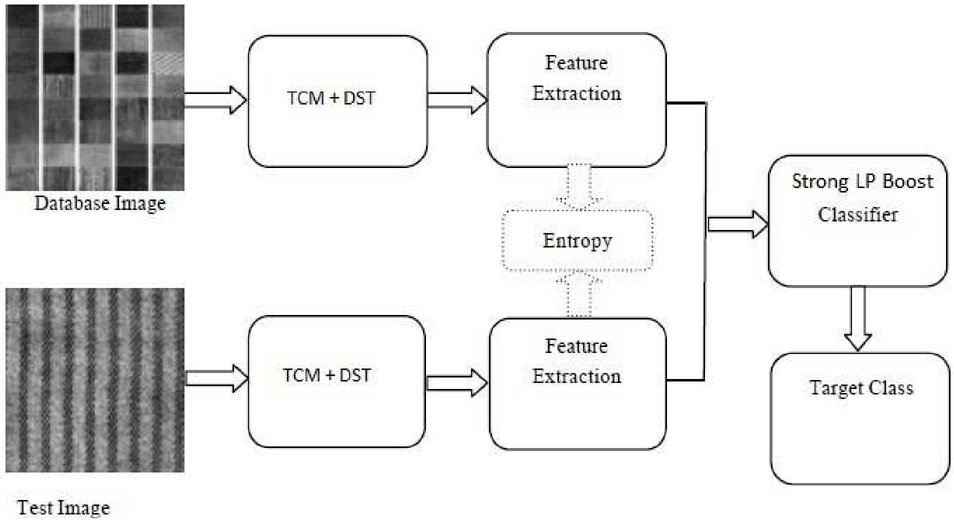

Fig. 3: The proposed system diagram

The texton image T with the adjacent pixels $P_1 = (x_1, y_1)$ as well as $P_2 = (x_2, y_2)$ and its corresponding weight of the pixels are $T(P_1) = w_1$ and $T(P_2) = w_2$. Similarly, the orientation angle of the image indicated as $\theta(P_1) = v_1$ and $\theta(P_2) = v_2$ Then, the group of texton image are undergoes to shearlet transform that decompose the image.

DISCRETE SHEARLET TRANSFORM

The most significant step of any classification system is feature extraction. A new shearlet band signature, entropy is proposed based on discrete shearlet transform introduced by Easley *et al*. (2008). The group of $N*N$ database image that derived from the above texton sub space image. It consists of a finite sequence of values, $\{x[n_1,n_2]_{n_1,n_2=0}^{N-1,N-1}\}$ where $N \in \mathbb{N}$. Identifying the domain with the finite group $\mathbb{Z}^2_N$, the inner product of image x, y: $\mathbb{Z}^2_N \rightarrow \mathbb{C}$ is defined as:

$$(x,y) = \sum_{u=0}^{N-1}\sum_{v=0}^{N-1} x(u,v)\overline{y(u,v)} \quad (8)$$

Thus the discrete analog of $L^2(\mathbb{R}^2)$ is $l^2\mathbb{Z}^2_N$. Given an image $f \in l^2(\mathbb{Z}^2_N)$, let $\hat{f}[k_1,k_2]$ denote its 2D Discrete Fourier Transform (DFT):

$$\hat{f}[k_1,k_2] = \frac{1}{N}\sum_{n_1,n_2=0}^{N-1} f[n_1,n_2]e^{-2\Pi i(\frac{n_1}{N}k_1+\frac{n_1}{N}k_2)} \quad (9)$$

The brackets in the equations $[\cdot,\cdot]$ denote arrays of indices and parentheses $(\cdot,\cdot)$ denote function evaluations. Then the interpretation of the numbers $\hat{f}[k_1,k_2]$ as samples $\hat{f}[k_1,k_2] = \hat{f}(k_1,k_2)$ is given by the following equation from the trigonometric polynomial:

$$\hat{f}(\xi_1,\xi_2) = \sum_{n_1,n_2=0}^{N-1} f[n_1,n_2]e^{-2\Pi i(\frac{n_1}{N}\xi_1+\frac{n_1}{N}\xi_2)} \quad (10)$$

First, to compute:

$$\hat{f}(\xi_1,\xi_2)\overline{V(2^{-2j}\xi_1,2^{-2j}\xi_2)} \quad (11)$$

In the discrete domain, at the resolution level j, the Laplacian pyramid algorithm is implemented in the time domain. This will accomplish the multi scale partition by decomposing $f_a^{j-1}[n_1,n_2], 0 \le n_1,n_2 < N_j - 1$ into a low pass filtered image $f_a^j[n_1,n_2]$, a quarter of the size of $f_a^{j-1}[n_1,n_2]$ and a high pass filtered image $f_d^{j-1}[n_1,n_2]$. Observe that the matrix $f_a^{j-1}[n_1,n_2]$ has size $N_j * N_j$, where $N_j = 2^{-2j}N$ and $f_a^0[n_1,n_2]$ is equal to $[n_1,n_2]$ has size $N*N$. In particular:

$$\hat{f}_d^j(\xi_1,\xi_2) = \hat{f}(\xi_1,\xi_2)\overline{V(2^{-2j}\xi_1,2^{-2j}\xi_2)} \quad (12)$$

Thus, $f_d^j[n_1,n_2]$ are the discrete samples of a function $f_d^j[x_1,x_2]$ whose Fourier transform is $\hat{f}_d^j(\xi_1,\xi_2)$. In order to obtain the directional localization the DFT on the pseudo-polar grid is computed and then one-dimensional band-pass filter is applied to the components of the signal with respect to this grid. More precisely, the definition of the pseudo-polar co-ordinates $(u, v) \in \mathbb{R}^2$ as follows:

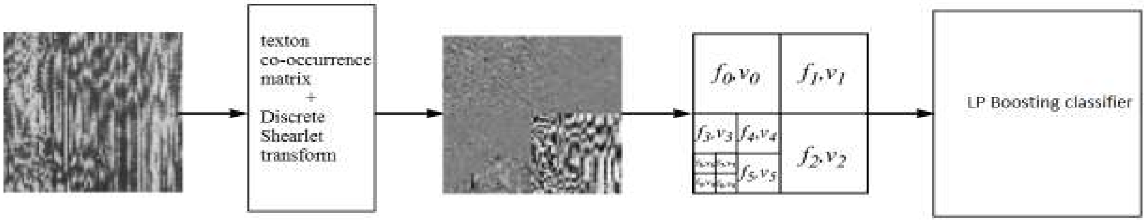

Fig. 4: The process of brodatz database image decomposition through TCM and DST

$$(u,v) = (\xi_1, \frac{\xi_2}{\xi_1}), if\,(\xi_1, \xi_2) \in D_0 \quad (13)$$

$$(u,v) = (\xi_1, \frac{\xi_1}{\xi_2}), if\,(\xi_1, \xi_2) \in D_1 \quad (14)$$

After performing this change of co ordinates, $g_j\,(u,v) = \hat{f}_d^j\,(\xi_1, \xi_2)$ is obtained and for $l = 1-2^j, ...2^j - 1$:

$$\hat{f}(\xi_1, \xi_2) = \overline{V(2^{-2j}\xi_1, 2^{-2j}\xi_2) W_{jl}^{(d)}(\xi_1, \xi_2)} \quad (15)$$
$$= g_j(u,v)\overline{W(2^j v - l)}$$

This expression shows that the different directional components are obtained by simply translating the window function W. The discrete samples $g_j[n_1, n_2] = g_j(n_1, n_2)$ are the values of the DFT of $f_d^j[n_1, n_2]$ on a pseudo-polar grid. That is, the samples in the frequency domain are taken not on a Cartesian grid, but along lines across the origin at various slopes. This has been recently referred to as the pseudo-polar grid. One may obtain the discrete Frequency values of f^j_d on the pseudo-polar grid by direct extraction using the Fast Fourier Trans-form (FFT) with complexity ON^2 log N or by using the Pseudo-polar DFT (PDFT). The upshot of the transformed image sequence in shown in the Fig. 4.

STRONG LPBOOST CLASSIFIER

The boosting classifier optimizes the classification based on edges "γ". The LP boost strong classifier focus on the weak classifier for the extracted features based on the shearlet transform relative entropy. It bounds as the edges of the strong classifier in which "γ" are lesser for minimum edges based on the convergence rate. The distributions of the edge margin are linear for training the set of images based on the similar features. The entropy regularized parameters for the feature vector, η to update the distribution clearly. Based on the mini-max theory that eliminates the error in classifying though error matrix that shown in Fig. 5.

	h_1	...	h_n	$\overline{d}$
x_1	$u_{1,1}$	...	$u_{1,n}$	d_1
...	...	...	...	...
x_m	$u_{m,1}$	...	$u_{1,n}$	d_n
$\overline{w}$	w_1	...	w_n	

Fig. 5: Error matrix in the training sets

In the Error matrix, the training sets X = {x_1, x_2, x_3…x_m} and $\bar{d}$ is the distribution of various training sets from d_1, d_2, d_3…d_n with the distribution of the hypothesis $\bar{w}$ from w_1, w_2, w_3…w_n that based on the features that manipulated with the hypothesis for each sample sets h_1, h_2, h_3…h_n. The mini-max theory suggests the edge constraints $\sum_{i=1}^{m} H'_{t-1}\,(x_i)$ based on its relative entropy through the feature extracted region. It helps to solve the weak classifier optimization effectively:

$$\begin{aligned}
& f^t(x) = \sum_{q=1}^{t} w_q h^q(x). \\
& \min_{d_t, \gamma} \gamma + \eta . \Delta\left(\overline{d}_t,\ \overline{d}_0\right) \\
& s.t \sum_{i=1}^{m} u_{i,j} d_i \le \gamma,\ \text{for } 1 \le \text{j} \le \text{t}; \\
& \sum_{i=1}^{m} H'_{t-1}(x_i)\, \text{y}_i\, d_i \le \gamma; \\
& 0 \le d_j \le \frac{v}{m}, \sum_j d_j = 1;
\end{aligned} \quad (16)$$

The main advantages of using LPboost classifiers are it performs train sequentially for the weak classifiers based on the preceding rules. It reduces the complication based on its hypotheses that based on Hinrichs *et al*. (2009).

RESULTS AND DISCUSSION

The performance evaluations of the proposed texture classification system are identified. From each original image, 128×128 pixel sized images are extracted with an overlap of 32 pixels between vertical and horizontal direction. From a single 640×640 texture

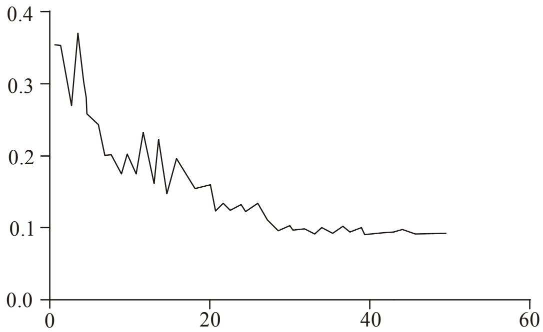

Fig. 6: The misclassification to the weak classifier in LPboosting classifier

image, 256 128×128 images are obtained. To carry out the proposed algorithm, 81 images are randomly selected from the 256 images. Among the 81 images, 40 images are randomly chosen to train the classifier and the remaining images are used to test the classifier. It shows the 2 and 3-level shearlet transform used to decompose the texture images by varying the number of directions from 2 to 64. Since the image are generated based on texton the DST is able to capture more information at higher directions. For 2-level decomposition, the classification accuracy increases from 92.87% (2 directions) to 99.82% (32 directions). The maximum classification accuracy achieved by 3-level decomposition with 32 directions is 99.85%. The Brodatz texture images are the systematic repetitive pattern of sequence and the proposed method enumerates the sub band in both the testing and training sets of images to analyze the homogeneous nature of images. By applying the TCM, the sub band of decomposition transform sequence are identified very accurately. It iterated at various levels for uniformly decompose the images into equally spatial blocks. The Brodatz test images are divvied into various classes to generalize the texture classification experiment. The discriminate functions based on the LPboosting classification reduce the redundancy and misclassification. Based on the error matrix, the misclassification reduced with constant iteration that shown in the Fig. 6.

The classification rates abruptly increases as the training sets feature increases. It predominantly shows the efficient classification in the training images. Similarly, the collection of test images which identified by the subset homogenous pattern for classification. It improves the calculation and classification performance which shown in the Fig. 7.

Table 1 shows the comparative analysis of the proposed system with other techniques in the literature in terms of classification accuracy (Fig. 8).

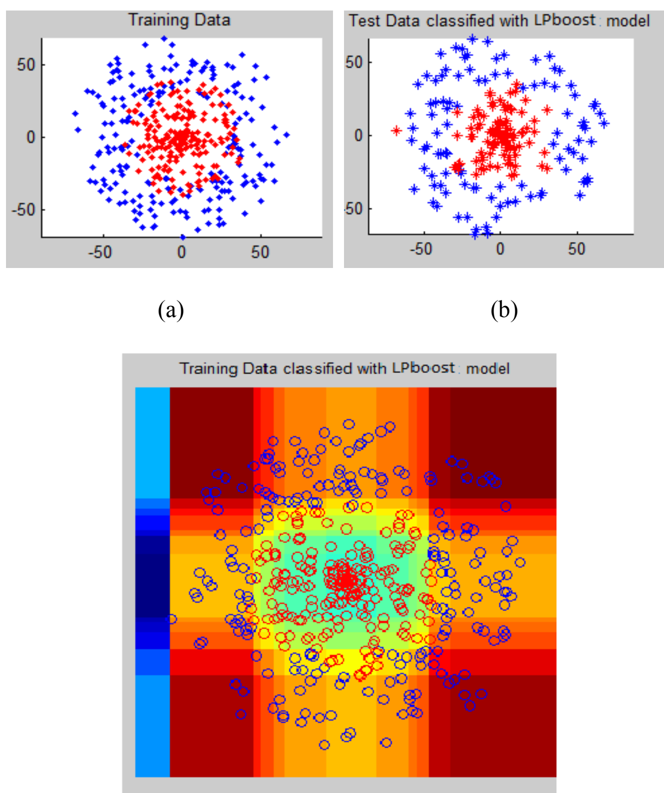

(a) (b)

(c)

Fig. 7: LPboosting classification on the texture images, (a) training data, (b) test data classified with LPboost model, (c) training data classified with LPboost model

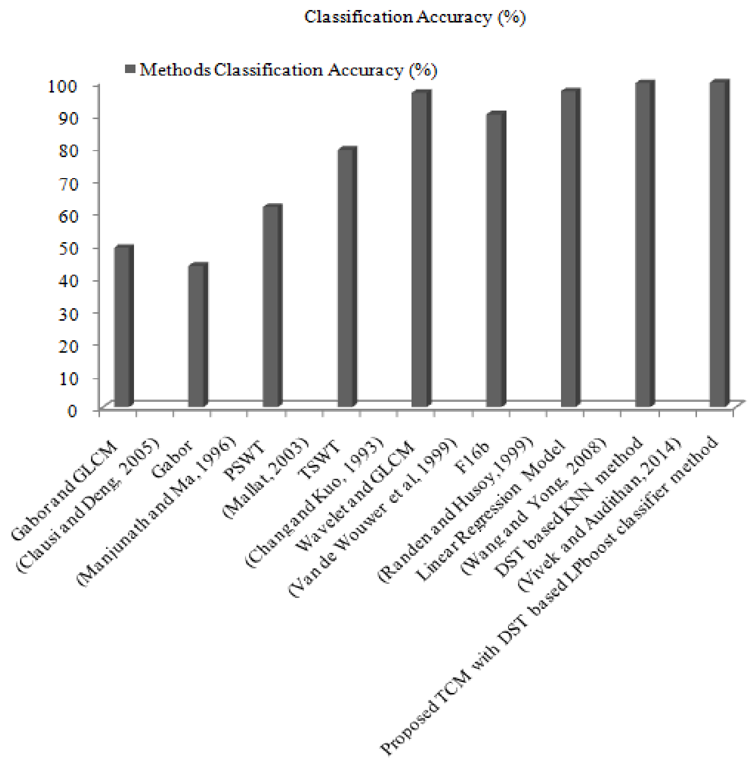

Fig. 8: Comparision graph of the propossed method

Table 1: Comparative analysis of the proposed system with other techniques

Methods	Wavelet and GLCM	(Van de Wouwer, 1998)	Linear regression model	(Wang and Yong, 2008)	DST based KNN method	(Vivek and Audithan, 2014)	Spatial co-occurrence and DST based texture classification using LPboosting classifier
Accuracy (%)	96.707		97.151		99.687		99.852

It is observed that the wavelet transform produces better performance than Gabor transform. Also the fusion of GLCM increases the classification accuracy. However, the proposed system based on DST outperforms all methods in terms of average classification accuracy.

CONCLUSION

In this study, the combination of texton co-occurrence matrix with shearlet band signatures based texture classification of 40 Brodatz texture images is presented. The feature extraction done more effectively and the sub-band are analyzed through the entropy measures and it undergoes for classification through LPboosting which provokes on weak classifier as the training images and then used to classify the testing images. The proposed system consistently achieves over 99.85% classification accuracy which is 0.16% higher than existing methods for accurate classification Experimental results show that the proposed TCM based DST outperforms Wavelet and Gabor transform based classification systems.

REFERENCES

Chen, C.H. and G.K. Young, 1982. A study of texture classification using spectral features. Technical Report F SMU-EE-TR-82-1.

Easley, G., D. Labate and W.Q. Lim, 2008. Sparse directional image representations using the discrete shearlet transform. Appl. Comput. Harmon. A., 25: 25-46.

Fang, Y., Y. Fu, C. Sun and J. Zhou, 2011. Improved boosting algorithm using combined weak classifiers. J. Comput. Inform. Syst., 7(5): 1455-1462.

Fang, Y.K., Y. Fu, C.J. Sun and J.L. Zhou, 2010. LPBoost with strong classifiers. Int. J. Comput. Intell. Syst., 3(Sup01): 88-100.

Haralick, R.M., K. Shanmugam and I.H. Dinstein, 1973. Textural features for image classification. IEEE T. Syst. Man Cyb., 6: 610-621.

Hinrichs, C., V. Singh, L. Mukherjee, G. Xu, M.K. Chung and S.C. Johnson, 2009. Spatially augmented LPboosting for AD classification with evaluations on the ADNI dataset. Neuroimage, 48(1): 138-149.

Julesz, B., 1981. Textons, the elements of texture perception and their interactions. Nature, 290: 91-97.

Liu, G.H., Z.Y. Li, L. Zhang and Y. Xu, 2011. Image retrieval based on micro-structure descriptor. Pattern Recogn., 44(9): 2123-2133.

Liu, G.H., L. Zhang, Y.K. Hou, Z.Y. Li and J.Y. Yang, 2010. Image retrieval based on multi-texton histogram. Pattern Recogn., 43(7): 2380-2389.

Monay, F. and D. Gatica-Perez, 2007. Modeling semantic aspects for cross-media image indexing. IEEE T. Pattern Anal., 29(10): 1802-1817.

Randen, T. and J.H. Husoy, 1999. Filtering for texture classification: A comparative study. IEEE T. Pattern Anal., 21(4): 291-310.

Smith, J.R. and S.F. Chang, 1994. Transform features for texture classification and discrimination in large image databases. Proceedings of the IEEE International Conference on Image Processing (ICIP-94), 3: 407-411.

Tou, J.Y., Y.H. Tay and P.Y. Lau, 2009. Recent trends in texture classification: A review. Proceedings of the Symposium on Progress in Information and Communication Technology. Kuala Lumpur, Malaysia, December 7-8.

Unser, M., 1986. Local linear transforms for texture measurements. Signal Process., 11(1): 61-79.

Unser, M., 1995. Texture classification and segmentation using wavelet frames. IEEE T. Image Process., 4(11): 1549-1560.

Van de Wouwer, G., 1998. Wavelets for multiscale texture analysis. Ph.D. Thesis, University of Antwerp, pp: 1-162.

Vivek, C. and S. Audithan, 2014. Texture classification by shearlet Band Signatures. Asian J. Sci. Res. Retrieved from: scialert.net/abstract/?doi=ajsr.0000.51616.51616.

Wang, Z.Z. and J.H. Yong, 2008. Texture analysis and classification with linear regression model based on wavelet transform. IEEE T. Image Process., 17(8): 1421-1430.